

ChemComm

Accepted Manuscript



This is an *Accepted Manuscript*, which has been through the Royal Society of Chemistry peer review process and has been accepted for publication.

Accepted Manuscripts are published online shortly after acceptance, before technical editing, formatting and proof reading. Using this free service, authors can make their results available to the community, in citable form, before we publish the edited article. We will replace this *Accepted Manuscript* with the edited and formatted *Advance Article* as soon as it is available.

You can find more information about *Accepted Manuscripts* in the [Information for Authors](#).

Please note that technical editing may introduce minor changes to the text and/or graphics, which may alter content. The journal's standard [Terms & Conditions](#) and the [Ethical guidelines](#) still apply. In no event shall the Royal Society of Chemistry be held responsible for any errors or omissions in this *Accepted Manuscript* or any consequences arising from the use of any information it contains.

Controllable Atmospheric Pressure Growth of Mono-layer, Bi-layer and Tri-layer Graphene

Cite this: DOI: 10.1039/x0xx00000x

Jing Li,^{ab} Hengxing Ji,^c Xing Zhang,^{ab} Xuanyun Wang,^d Zhi Jin,^d Dong Wang*^a and Li-Jun Wan*^a

Received 00th January 2012,
Accepted 00th January 2012

DOI: 10.1039/x0xx00000x

www.rsc.org/

Here we report a three-step growth method for high-quality mono-layer, bi-layer and tri-layer graphene with coverage higher than 90% at atmospheric pressure. The growth temperature and gas flow rate are found to be the key factors. This method would be of great importance for the large scale production of graphene with defined thickness.

Owing to its outstanding physical properties like superb carrier mobility, specific surface area, and so forth,¹ graphene has been regarded as the next generation of materials since its discovery on dielectric substrate by mechanical exfoliation.² In 2009, the single-layer graphene with more than 95% coverage on copper with arbitrary size was synthesized by chemical vapor deposition (CVD).³ This large scale production of high quality graphene film further attracts ever-growing interests of graphene application, especially for electronic devices.⁴

Though charming as single layer graphene might be, its semimetal and zero band-gap electronic structure limits its further electronic and optical applications.⁵ It has been demonstrated that the Bernal-stacking bilayer graphene has a variable external electric field tuned band gap, which is highly desirable for electronic device application.^{6,7} Since then, great efforts have been devoted to grow high quality graphene with controlled thickness and stacking mode.^{8,9} Low-pressure CVD (LPCVD) has been proven to be an effective way to synthesis graphene on Cu with controlled thickness due to the long free-path diffusion length and high diffusivity of active carbon species at low pressure, which is favorable for graphene ad-layer nucleation and growth with the existing of pre-grown graphene sheet.¹⁰⁻¹² For example, Liu et al.¹³ and Duan et al.⁵ obtained bi-layer graphene with coverage from 67% to 95%. Tour's group has obtained graphene films with thickness of 2- to 4-layers by controlling total pressure and the component ratio of growth gases.¹⁴ On the other hand, atmospheric pressure CVD (APCVD) has been proven to be an effective alternative to grow high-quality monolayer graphene on copper substrate and to control the grain boundaries.^{15,16} The hexagonal shape of single crystalline graphene domain that is usually obtained by APCVD is favorable for minimizing the defects formed when two crystalline domains are merged together.¹⁷ Moreover, APCVD technique is practically more suitable for roll-to-roll process which is of great interest for industrial application. However, the layer number control of graphene for APCVD is more

difficult than that for LPCVD as a result of the shorter mean free-diffusive path of the active carbon species at atmospheric pressure.

Herein, we report a coherent three-step growth method for controllable synthesis of high quality single-layer, bi-layer and tri-layer graphene with APCVD. The growth temperature and gas flow rate are found to be the two key factors in graphene layer number control. Under the optimized growth conditions, the coverage of bi-layer and tri-layer graphene can both reach ~90% on the Cu foil. The intermediate state of the tri-layer graphene is studied, and the results suggest that the graphene layers nucleate at the same stage and grow with the same rate. This result would be of great interest for potential large-scale multilayer graphene production.

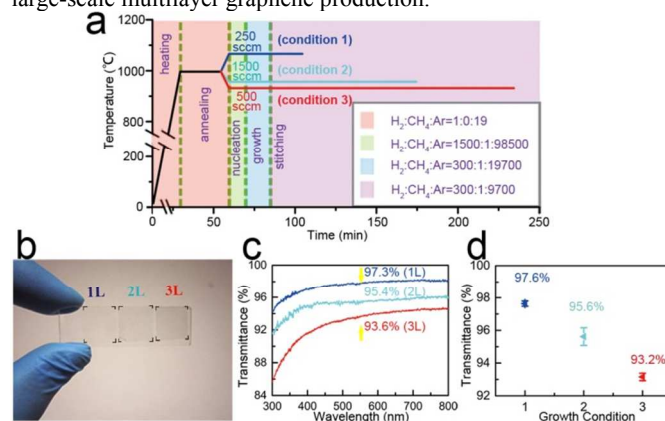


Fig 1. (a) Progress diagram of graphene growth parameters dependence on time: temperature, gas composition/flow rate. The lower insert is the concentration ratio of different gas flow in each growth stage. The photograph (b) and UV-vis transmittance (c) of as grown mono- to tri-layer graphene on quartz substrate. (d) Growth condition dependent UV-vis spectroscopy of as-prepared graphene on quartz substrate.

First, we investigate the effect of growth temperature and gas flow rate on the layer number of APCVD graphene. The growth temperature was tuned in the range of 900 to 1070 °C, and the total gas flow rate was tuned in the range of 250 to 1500 standard cubic centimeters per minute (sccm), respectively. Scanning electron microscopy (SEM) images (Figure S1, S2 and S3) of graphene on

Cu indicate that the graphene ad-layers increase with lower growth temperature or higher total gas flow rate. To control the graphene coverage, a three-step growth process was applied. The total gas flow rate and CH₄/H₂ gas ratio at each growth stage are shown in Figure 1a. The first step was nucleation. At this stage, low partial pressure of CH₄ was controlled at temperature of 1070, 960 and 930 °C, respectively. We anticipate that graphene nuclei with different layers could be formed as the lower growth temperature yields more graphene layers (Figure S1 and S2). The next step was to enlarge the graphene domain. The CH₄ partial pressure was increased by a factor 5 while maintaining the predefined temperatures of 1070, 960, and 930 °C for single-layer, bi-layer, and tri-layer graphene, respectively. Finally in the stitching step, the partial pressure of both the CH₄ and H₂ were doubled by decreasing Ar flow rate to assist individual graphene domains to merge together. Under the optimized growth parameters labelled in Figure 1a, we obtained single-layer (at condition 1), bi-layer (at condition 2) and tri-layer (at condition 3) graphene with coverage of up to 90%.

The graphene films were transferred onto quartz substrate with wet-transfer method.¹⁸ The optical microscopy images of graphene film grown at conditions 1, 2 and 3 (Figure 1b) show visible transmittance difference. The UV-Vis spectroscopy measurement (Figure 1c and 1d) indicates that the transmittance values at 550 nm incidence light are 97.6 ± 0.2 , 95.6 ± 0.5 and $93.2 \pm 0.2\%$, for graphene films obtained at growth conditions of 1, 2 and 3, respectively. According to previous reports,¹⁹ the theoretical transmittance of single layer graphene is 97.7 %, and multilayer stacking will result in linear attenuation of transmittance with a gradient of 2.3% per layer.²⁰ Therefore, the graphene films we obtained are single-layer, bi-layer and tri-layer with relevant large area (Figure 1b and 1c) and high uniformity (Figure 1d).

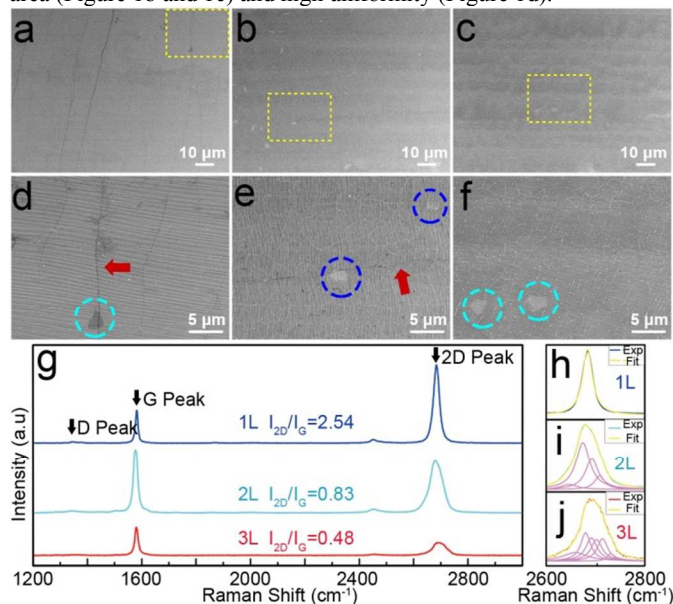


Fig 2. (a-c) The large scale SEM images of graphene with different thickness grown by optimized growth condition 1, 2 and 3, respectively. (d-f) The zoom-in SEM images taken at the yellow-dashed box region in panel (a), (b) and (c), respectively. The cyan and blue dash circles marks bi-layer and single-layer graphene, respectively, and the red arrow indicates the wrinkle of graphene. (g) Raman spectroscopy of mono-, bi- and tri-layer graphene films on SiO₂/Si substrate. (h-j) The Lorentzian curve fitted 2D peaks of mono-, bi- and tri-layer graphene films in panel (g), respectively.

The uniformity of graphene films on Cu were further investigated with SEM (Figure 2a-f). The low magnification SEM images of graphene on Cu grown at condition 1 (Figure 2a), condition 2 (Figure 2b) and condition 3 (Figure 2c) all show uniform contrast except for darker lines, and some darker or lighter islands with low coverage (Figure 2d-f), indicative of uniform coverage of graphene film. The dark lines are graphene wrinkles.^{3, 21} The blue Raman spectrum acquired on samples grown at condition 1 has an I_{2D}/I_G ratio of higher than 2. And the 2D peak can be fitted with one Lorentzian curve with full width at half maximum (FWHM) of about 27 cm⁻¹ (Figure 2g and h), indicating that the monolayer graphene is grown on Cu foil.³ The cyan Raman spectrum acquired on sample grown at condition 2 has an I_{2D}/I_G ratio of approximately 1 (Figure 2g) and a 2D peak FWHM of about 52 cm⁻¹ (Figure 2i).^{5, 13} The red Raman spectrum acquired on samples grown at condition 3 has an I_{2D}/I_G ratio of about 0.5 (Figure 2g) and a 2D peak FWHM of about 63 cm⁻¹ grown at condition 3 has an I_{2D}/I_G ratio of about 0.5 (Figure 2g) and a 2D peak FWHM of about 63 cm⁻¹ (Figure 2j). These Raman features fit that of bi-layer and tri-layer graphene.²²

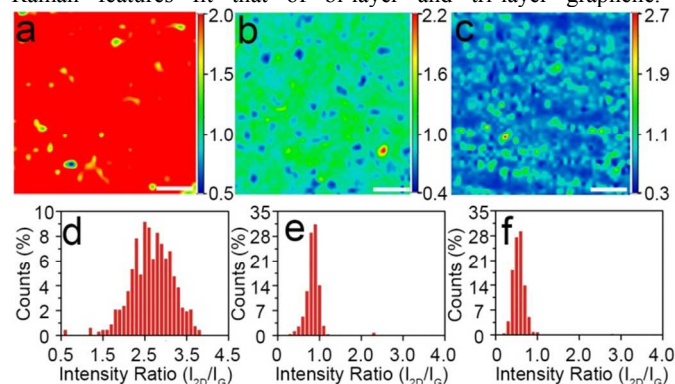


Fig 3. (a-c) Raman mapping images of mono-, bi- and tri-layer graphene films on SiO₂/Si substrate. (d-f) Statistics of I_{2D}/I_G in Raman mapping from panel (a)-(c), respectively. Scale bar in panel (a)-(c) is 10 μm.

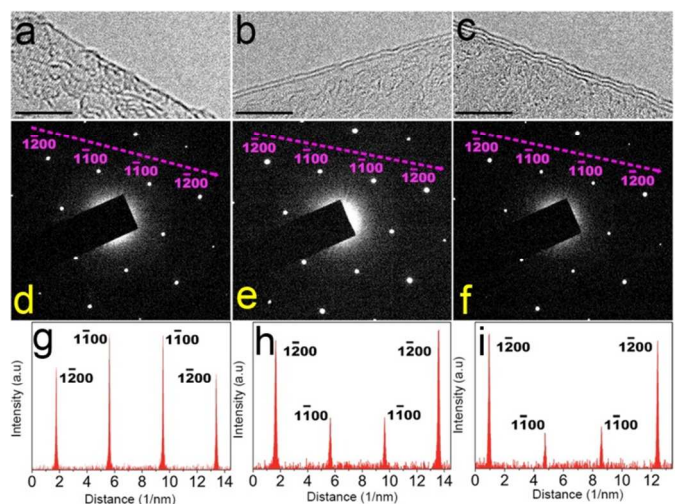


Fig 4. HRTEM and SAED characterization of as-prepared mono-, bi- and tri-layer graphene. (a-c) High resolution TEM of randomly chosen edge of mono-, bi- and tri-layer graphene, respectively. (d-f) SAED pattern of graphene from panel (a-c), respectively. (g-i) Intensity profile along the direction marked in SAED patterns in panel (d-f). Scale bar in panel (a-c) is 5nm.

The Raman mapping measured at a $50 \times 50 \mu\text{m}^2$ area (Figure 3a-c) and the statistics of the I_{2D}/I_G ratio of the graphene film transferred

on Si/SiO₂ after growing at condition 1, 2 and 3 (Figure 3d-f) indicate a uniform dispersion of the graphene thickness. In addition, we used a Cu strip of 6.0 cm-long to grow graphene at conditions 1, 2 and 3, respectively. SEM images and UV-Vis spectra show nondetectable difference of graphene grown at different positions of this long Cu stripe (Figure S4 and S5).

The graphene films were transferred onto TEM grids and characterized by high resolution transmission electron microscopy (HRTEM) and selected area electron diffraction (SAED).²³ The HRTEM images of graphene edge chosen arbitrarily from the samples grown at condition 1, 2 and 3 are shown in Figure 4a-c, respectively, which reveal the single-layer, bi-layer and tri-layer nature. Moreover, we acquired tens of SAED patterns randomly selected at different positions per graphene sample (Figure 4d-e). About 80% of the measurements show one set of SAED pattern, among which the intensity ratio between ($1\bar{2}10$) and ($1\bar{1}00$) spots (Figure 4g-i) are 0.75, 2.61, and 4.00, respectively, for graphene grown at condition 1, 2 and 3, in consistence with the single-layer, bi-layer and tri-layer Bernal-stacked graphene.^{12, 14} In addition, the electrical measurement on the dual-gate field effect transistor of as-prepared bi-layer graphene shows tunable band structure with different displacement field, which indicates that the graphene is Bernal structure.¹³ The carrier mobility is about 1300 cm²V⁻¹S⁻¹, which is comparable to those reported previously,^{13, 14} reasonably demonstrating the as-prepared graphene is of good-quality (Figure S6).

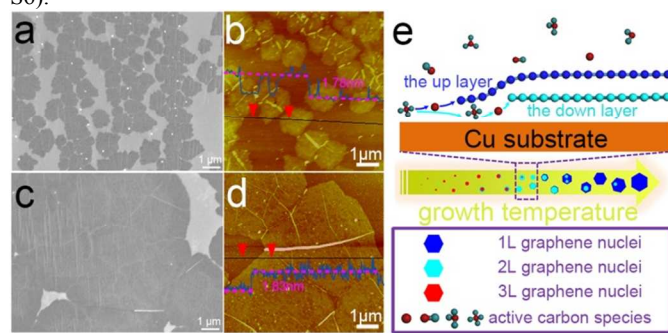


Fig 5. The intermediate states of tri-layer graphene on Cu substrate under the growth condition 3, which was stopped after nucleation step (a-b) and growth step (c-d), respectively. The vertical height distance profile along the black line is inserted in panel (b) and (d), respectively. e) The proposed growth-mechanism for multi-layers graphene growth.

To better understand the mechanism of the graphene growth, the growth of tri-layer graphene were stopped after the nucleation and growth stages, respectively (Figure 5a-b). The result indicates that the tri-layer graphene grown at condition 3 was initiated by a nucleation center having three layers, and the growth rate of the graphene layers stacked at different levels of the tri-layer graphene are almost the same. It is reported that the concentration and migration rate of active carbon species²⁴ play dominant roles for the graphene domain extension rate. Generally, the graphene ad-layers grow under the top graphene-layer with slower growth rate because of the high diffusion barrier of the carbon species at graphene domain boundaries where the top graphene edge touches the Cu substrate.²⁵ However, the hydrogen terminated graphene edge could lower such barrier, thus, accelerate the bottom-layer growth under the top-layer.²⁶ In this study, we found that the temperature is the key parameter to control the stacked graphene layer number. This is very likely because the more stable hydrogen-carbon bond at lower temperature minimizes the diffusion barrier for active carbon species to transfer under the top-layer. Thus under an optimum growth

temperature and gas flow rate, the growth of up- and low-layer graphene can be balanced to obtain uniform multi-layer graphene (Figure 5e).

In summary, we developed a coherent three-step growth method by using APCVD, and obtained mono-, bi- and tri-layer graphene with coverage of ~90%, respectively, on the Cu foil. The growth temperature and gas flow rate are found to be the key factors. The intermediate states of the tri-layer graphene obtained by stop growing after the nucleation and growth stage suggest that the graphene layers nucleate at the same stage and grow with a same rate. This method would be of great importance for the large scale production of graphene with defined thickness.

This work was supported by the National Key Project on Basic Research (Grants 2011CB808700, 2011CB932300), National Natural Science Foundation of China (21121063, 21127901, 61136005), and the Strategic Priority Research Program of the Chinese Academy of Sciences (Grant No. XDB12020100).

Notes and references

^a Key Laboratory of Molecular Nanostructure and Nanotechnology and Beijing National Laboratory for Molecular Sciences, Institute of Chemistry, Chinese Academy of Sciences (CAS), Beijing 100190, P.R. China

E-mail: wangd@iccas.ac.cn; wanlijun@iccas.ac.cn

^b University of CAS, Beijing100049, P. R. China

^c Department of Materials Science&Engineering
University of Science and Technology of China
96 Jinzhai Road, Hefei, Anhui 230026, P.R. China

^d Institute of Microelectronics, Chinese Academy of Sciences, Beijing 100029, P. R. China

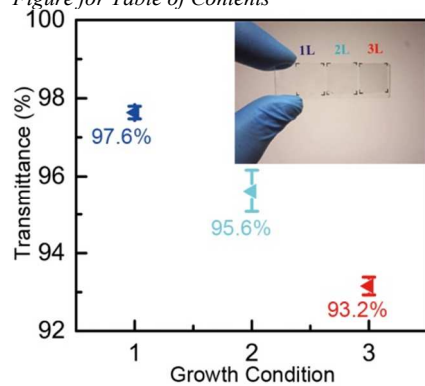
† Electronic Supplementary Information (ESI) available. See DOI: 10.1039/c000000x/

1. F. Schedin, A. K. Geim, S. V. Morozov, E. W. Hill, P. Blake, M. I. Katsnelson and K. S. Novoselov, *Nat Mater*, 2007, **6**, 652-655.
2. K. S. Novoselov, A. K. Geim, S. V. Morozov, D. Jiang, Y. Zhang, S. V. Dubonos, I. V. Grigorieva and A. A. Firsov, *Science*, 2004, **306**, 666-669.
3. X. S. Li, W. W. Cai, J. H. An, S. Kim, J. H. Nah, D. X. Yang, R. Piner, A. Velamakanni, I. Jung, E. Tutuc, S. K. Banerjee, L. Colombo and R. S. Ruoff, *Science*, 2009, **324**, 1312-1314.
4. T. Kobayashi, M. Bando, N. Kimura, K. Shimizu, K. Kadono, N. Umez, K. Miyahara, S. Hayazaki, S. Nagai, Y. Mizuguchi, Y. Murakami and D. Hobar, *Appl. Phys. Lett.*, 2013, **102**, 023112-023114.
5. L. X. Liu, H. L. Zhou, R. Cheng, W. J. Yu, Y. Liu, Y. Chen, J. Shaw, X. Zhong, Y. Huang and X. F. Duan, *ACS Nano*, 2012, **6**, 8241-8249.
6. Y. B. Zhang, T.-T. Tang, C. Girit, Z. Hao, M. C. Martin, A. Zettl, M. F. Crommie, Y. R. Shen and F. Wang, *Nature*, 2009, **459**, 820-823.
7. M. Aoki and H. Amawashi, *Solid State Commun.*, 2007, **142**, 123-127.
8. C.-C. Lu, Y.-C. Lin, Z. Liu, C.-H. Yeh, K. Suenaga and P.-W. Chiu, *ACS Nano*, 2013, **7**, 2587-2594.
9. A. W. Robertson and J. H. Warner, *Nano Letters*, 2011, **11**, 1182-1189.
10. Z. Peng, Z. Yan, Z. Sun and J. M. Tour, *ACS Nano*, 2011, **5**, 8241-8247.

11. Z. Yan, Z. Peng, Z. Sun, J. Yao, Y. Zhu, Z. Liu, P. M. Ajayan and J. M. Tour, *ACS Nano*, 2011, **5**, 8187-8192.
12. S. Lee, K. Lee and Z. H. Zhong, *Nano Letters*, 2010, **10**, 4702-4707.
13. K. Yan, H. L. Peng, Y. Zhou, H. Li and Z. F. Liu, *Nano Letters*, 2011, **11**, 1106-1110.
14. Z. Z. Sun, A.-R. O. Raji, Y. Zhu, C. S. Xiang, Z. Yan, C. Kittrell, E. L. G. Samuel and J. M. Tour, *ACS Nano*, 2012, **6**, 9790-9796.
15. D. C. Geng, B. Wu, Y. L. Guo, L. P. Huang, Y. Z. Xue, J. Y. Chen, G. Yu, L. Jiang, W. P. Hu and Y. Q. Liu, *Proc. Nat. Acad. Sci. U.S.A.*, 2012, **109**, 7992-7996.
16. Z. Yan, J. Lin, Z. W. Peng, Z. Z. Sun, Y. Zhu, L. Li, C. S. Xiang, E. L. Samuel, C. Kittrell and J. M. Tour, *ACS Nano*, 2012, **6**, 9110-9117.
17. J.-H. Lee, E. K. Lee, W.-J. Joo, Y. Jang, B.-S. Kim, J. Y. Lim, S.-H. Choi, S. J. Ahn, J. R. Ahn, M.-H. Park, C.-W. Yang, B. L. Choi, S.-W. Hwang and D. Whang, *Science*, 2014, **344**, 286-289.
18. I. N. Kholmanov, C. W. Magnuson, A. E. Aliev, H. F. Li, B. Zhang, J. W. Suk, L. L. Zhang, E. Peng, S. H. Mousavi, A. B. Khanikaev, R. Piner, G. Shvets and R. S. Ruoff, *Nano Letters*, 2012, **12**, 5679-5683.
19. W. Ying Ying, G. Ren Xi, N. Zhen Hua, H. Hui, G. Shu Peng, Y. Huan Ping, C. Chun Xiao and Y. Ting, *Nanotechnology*, 2012, **23**, 495713.
20. X. Li, Y. Zhu, W. Cai, M. Borysiak, B. Han, D. Chen, R. D. Piner, L. Colombo and R. S. Ruoff, *Nano Letters*, 2009, **9**, 4359-4363.
21. N. Liu, Z. H. Pan, L. Fu, C. H. Zhang, B. Dai and Z. F. Liu, *Nano Research*, 2011, **4**, 996-1004.
22. A. C. Ferrari, J. C. Meyer, V. Scardaci, C. Casiraghi, M. Lazzeri, F. Mauri, S. Piscanec, D. Jiang, K. S. Novoselov, S. Roth and A. K. Geim, *Phys. Rev. Lett.*, 2006, **97**, 187401.
23. J. C. Meyer, A. K. Geim, M. I. Katsnelson, K. S. Novoselov, T. J. Booth and S. Roth, *Nature*, 2007, **446**, 60-63.
24. H. Chen, W. G. Zhu and Z. Y. Zhang, *Phys. Rev. Lett.*, 2010, **104**, 186101.
25. Q. Y. Li, H. Chou, J. H. Zhong, J. Y. Liu, A. Dolocan, J. Zhang, Y. H. Zhou, R. S. Ruoff, S. Chen and W. W. Cai, *Nano Letters*, 2013, **13**, 486-490.
26. X. Y. Zhang, L. Wang, J. Xin, B. I. Yakobson and F. Ding, *J. Am. Chem. Soc.*, 2014, **136**, 3040-3047.

Journal Name

Figure for Table of Contents



A coherent three-step growth method has been developed for mono-, bi- and tri-layer graphene with coverage of ~90% at atmospheric pressure on Cu foil.